the plant journal

SEB Society for Experimental Biology

The Plant Journal (2017) **92,** 263–275 doi: 10.1111/tpj.13650

miR3954 is a trigger of phasiRNAs that affects flowering time in citrus

Yuanlong Liu[1,†], Lili Ke[1,†], Guizhi Wu[1], Yuantao Xu[1], Xiaomeng Wu[1], Rui Xia[2], Xiuxin Deng[1] and Qiang Xu[1,*]

[1]*Key Laboratory of Horticultural Plant Biology of Ministry of Education, Huazhong Agricultural University, Wuhan 430070, China, and*

[2]*State Key Laboratory for Conservation and Utilization of Subtropical Agro-Bioresources, Guangzhou 510642, China*

Received 3 March 2017; revised 20 July 2017; accepted 25 July 2017; published online 27 July 2017.

*For correspondence (e-mail xuqiang@mail.hzau.edu.cn).

†These authors contributed equally to this work.

SUMMARY

In plant, a few 22-nt miRNAs direct cleavages of their targets and trigger the biogenesis of phased small interfering RNAs (phasiRNAs) in plant. In this study, we characterized a miRNA triggering phasiRNAs generation, miR3954, and explored its downstream target genes and potential function. Our results demonstrated that miR3954 showed specific expression in the flowers of citrus species, and it targeted a *NAC* transcription factor (*Cs7 g22460*) and two non-coding RNA transcripts (lncRNAs, *Cs1 g09600* and *Cs1 g09635*). The production of phasiRNAs was detected from transcripts targeted by miR3954, and was further verified in both sequencing data and transient expression experiments. PhasiRNAs derived from the two lncRNAs targeted not only miR3954-targeted *NAC* gene but also additional *NAC* homologous genes. No homologous genes of these two lncRNAs were found in plants other than citrus species, implying that this miR3954-lncRNAs-phasiRNAs-*NAC* pathway is likely citrus-specific. Transgenic analysis indicated that the miR3954-overexpressing lines showed decreased transcripts of lncRNA, elevated abundance of phasiRNAs and reduced expression of *NAC* genes. Interestingly, the overexpression of miR3954 leads to early flowering in citrus plants. In summary, our results illustrated a model of the regulatory network of miR3954-lncRNA-phasiRNAs-*NAC*, which may be functionally involved in flowering in citrus.

Keywords: *Citrus sinensis*, miR3954, phasiRNAs, NAC transcription factor, regulatory network.

INTRODUCTION

In plants, microRNAs (miRNAs) with a length of 20–24 nucleotides (nt) play vital roles in development. Generally, miRNAs in plants with different lengths are generated through diverse biogenesis pathways and have different functions. In most cases, canonical miRNAs, which are generated by Dicer-like 1 (DCL1), cooperate with ARGONAUTE 1 (AGO1) proteins and constitute RNA-induced silencing complexes (RISCs) to guide posttranscriptional gene silencing through direct cleavage or translation inhibition of target mRNAs (Bartel, 2004; Vaucheret, 2008; Voinnet, 2009; Wang *et al.*, 2011). Phased small interfering RNAs (phasiRNAs), another major types of small RNAs in plants, were firstly reported in the model plant Arabidopsis, which were termed as trans-acting siRNAs (tasiRNA) initially, as these siRNAs are derived from non-coding transcripts and function *in trans* to target downstream genes (Peragine *et al.*, 2004; Vazquez *et al.*, 2004; Allen *et al.*, 2005; Yoshikawa *et al.*, 2005). In Arabidopsis, miR173 triggers the formation of tasiRNAs targeting pentatricopeptide repeat protein coding genes from *TAS1* and *TAS2*; miR828 targets *TAS4* and triggers the formation of tasiRNAs targeting *MYB* transcription factors (Rajagopalan *et al.*, 2006). miR390 triggers the biogenesis of tasiRNAs from *TAS3*, targeting genes encoding auxin response factor (ARF; Allen *et al.*, 2005).

Although a few 21-nt miRNAs, such as miR390 and miR161, were loaded into AGO7 and triggered the biogenesis of phasiRNAs (Axtell *et al.*, 2006; Montgomery *et al.*, 2008; Allen and Howell, 2010; Fei *et al.*, 2013), it has been widely reported that 22-nt miRNAs play a dominant role in triggering the biogenesis of phasiRNAs (Allen *et al.*, 2005; Allen and Howell, 2010; Chen *et al.*, 2010; Cuperus *et al.*, 2010). Most 22-nt miRNAs are derived from asymmetric miRNA/miRNA* duplexes that are likely processed by DCL1 (Cuperus *et al.*, 2010). After the direction of accurate slicing, 22-nt miRNAs cooperate with AGO1 to recruit RNA-

dependent RNA polymerase 6 (RDR6) to convert the 3′ cleaved fragment into double-stranded RNA (dsRNA; Cuperus *et al.*, 2010). Subsequently, DCL4 processes the dsRNA into 21-nt or 24-nt phasiRNAs in a sequential head-to-tail manner right after the miRNA cleavage site (Allen *et al.*, 2005; Xie *et al.*, 2005; Yoshikawa *et al.*, 2005, 2013; Johnson *et al.*, 2009; Allen and Howell, 2010; Cuperus *et al.*, 2010; Zhai *et al.*, 2015). Experimental evidence has demonstrated that increasing the length of a miRNA from 21 nt to 22 nt gave the miRNA a competence of triggering phasiRNAs biogenesis from its target genes (Chen *et al.*, 2010; Cuperus *et al.*, 2010).

With the biogenesis process of phasiRNAs essentially worked out, researchers developed bioinformatics approaches to detect extensive *PHAS* loci of phasiRNAs production and their miRNA triggers in several species, such as soybean, citrus, Norway spruce and strawberry (Xia *et al.*, 2013, 2015a,b; Arikit *et al.*, 2014; Liu *et al.*, 2014b; Wu *et al.*, 2015). To date, studies have indicated that phasiRNAs are involved in different biological processes, such as heat stress (Li *et al.*, 2014), plant defense responses (Zhai *et al.*, 2011; Li *et al.*, 2012; Fei *et al.*, 2013; Zhao *et al.*, 2015), secondary metabolite synthesis (Xia *et al.*, 2012; Rock, 2013), and especially plant development (Peragine *et al.*, 2004; Xie *et al.*, 2005; Liu *et al.*, 2007; Johnson *et al.*, 2009; Cho *et al.*, 2012; Lam *et al.*, 2015; Zhai *et al.*, 2015). In *Physcomitrella patens*, miR156 and miR390 co-target a *PHAS* transcript and co-modulate the accumulation of phasiRNAs that affect development timing (Cho *et al.*, 2012). After a combined data set of small RNAs from different tissues in rice was analyzed, 831 out of 1029 phasiRNAs were detected preferentially expressed in developing rice inflorescences, which suggests that these phasiRNAs function in early reproductive development in rice (Johnson *et al.*, 2009). In Arabidopsis, *dcl4*, *rdr6* and *sgs3* mutants that lack phasiRNAs display an accelerated transition from the juvenile to adult phase, indicating that phasiRNAs in Arabidopsis are involved in vegetative development (Peragine *et al.*, 2004; Xie *et al.*, 2005). All of these studies imply that phasiRNAs are likely involved in the regulation of the transition from vegetative to reproductive development.

Our earlier *in silico* analyses predicted that citrus miR472, miR482, miR827, miR3954 and miRN20 (also named as miR059) may have the potential to act as triggers of phasiRNAs (Liu *et al.*, 2014b; Wu *et al.*, 2015). A total of 407 potential *PHAS* loci were systematically predicted in citrus genome (Zheng *et al.*, 2015). In this study, we demonstrate that the 22-nt miR3954 targets a NAC transcript and two citrus-specific non-coding transcripts, triggering the biogenesis of phasiRNAs, which in turn regulates many other NAC homologs. Overexpression of miR3954 indicated that this pathway might be involved in the induction of early flowering in citrus.

RESULTS

Csi-miR3954 targets one *NAC* gene and two lncRNAs in citrus

Csi-miR3954, a 22-nt miRNA in *Citrus sinensis*, was identified by our previous high-throughput sequencing analysis (Xu *et al.*, 2010; Liu *et al.*, 2014b). *MIR3954* is a single-copy gene that was located in chromosome 9 of *C. sinensis*. The hairpin secondary structure of the miR3954 precursor was included in a 148-nt sequence. Within the hairpin structure, a bulge led to the generation of an asymmetric miRNA/miRNA* (22nt/21nt) duplex that yielded a 22-nt mature miR3954 (Figure 1a). RNA gel blots showed that miR3954 was highly expressed in the flowers of all four citrus species, including sweet orange (*C. sinensis*), pummelo (*Citrus grandis*), mandarin (*Citrus reticulata*) and Hongkong kumquat (*Fortunella hindsii*; Figure 1b). We hypothesized that the higher expression of miR3954 in flower might contribute to regulation of flower development or other reproductive traits. After analyzing the degradome sequencing data, *Cs7 g22460*, *Cs1 g09600* and *Cs1 g09635* were identified as target genes of miR3954. Furthermore, 5′-rapid amplification of cDNA ends (5′ RACE) analysis was carried out to detect the cleavage site of each target. As shown in Figure 1c, miR3954-mediated cleavage occurred in the complementary structure of all target genes between the 10th and 11th nucleotide relative to the 5′ end of miR3954, which was consistent with previous researches on miRNA-mediated degradation (Llave *et al.*, 2002; Mallory and Bouché, 2008; Liu *et al.*, 2014a). These data verified that miR3954 targeted the *Cs7 g22460*, *Cs1 g09600* and *Cs1 g09635 in vivo*. After manual annotation, *Cs7 g22460* was annotated as a *NAC* transcription factor, whereas *Cs1 g09600* and *Cs1 g09635* cannot be annotated as protein-coding genes. Then we evaluated the coding potential of *Cs1 g09600* and *Cs1 g09635* using an online tool (Coding Potential Calculator, http://cpc.cbi.pku.edu.cn/; Kong *et al.*, 2007). As a result, the largest predicted open reading frame of *Cs1 g09600* and *Cs1 g09635* encoded a 29-amino acids peptide (8.64% of the whole transcript) and a 25-amino acids peptide (8.13% of the whole transcript), respectively (Appendix S1). The predicted small peptides could not be detected in our previously published proteomics data (Pan *et al.*, 2009, 2012; Zheng *et al.*, 2014). Additionally, we used *Cs1 g09600* and *Cs1 g09635* as query sequences to BLASTN against the nucleotide collection (nr/nt) database; as a result, all significant alignments were from citrus. Considering that *Cs1 g09600* and *Cs1 g09635* genes do not have homologous protein-coding genes in other plant species and exhibit a very low confidence of protein-coding potential, we regarded these two genes as citrus-specific non-coding genes.

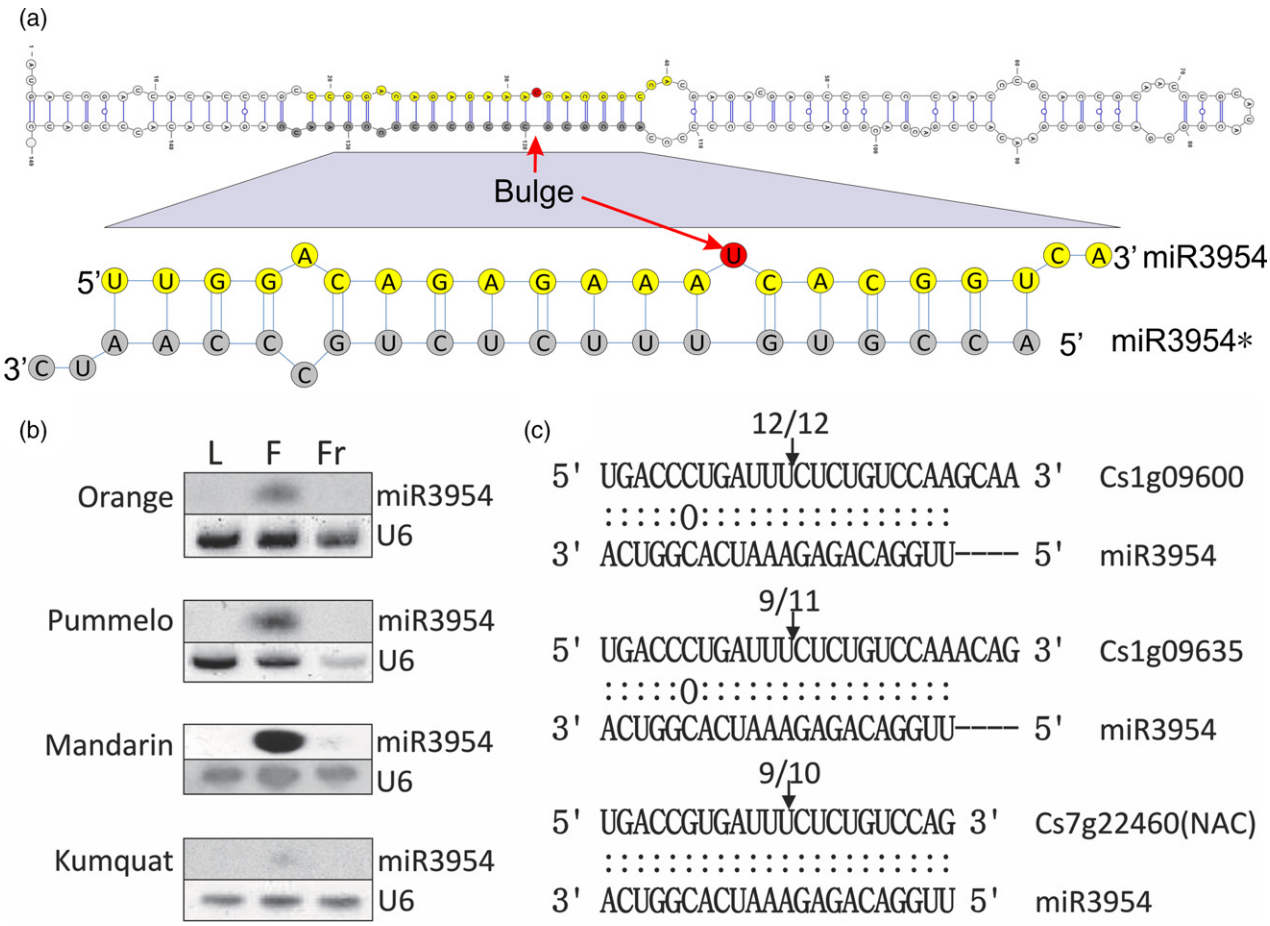

Figure 1. Precursor structure, expression pattern and target validation of miR3954.
(a) Secondary structure of pre-miR3954 from orange. The sequence of mature miR3954 is highlighted in yellow, whereas the miR3954* is in gray. The red arrow indicates the bulge in the miRNA/miRNA* duplex.
(b) The expression level of miR3954 in different tissues of different citrus species. The expression level of miR3954 was analyzed by an RNA gel blot in which snRNA U6 was used as a loading control. L, leaf; F, flower; Fr, fruit.
(c) Target validation was carried out using 5′ rapid amplification of cDNA ends (RACE) analysis. The arrows indicate the cleavage sites in each target and the numbers indicate the frequency of valid sequenced clones. [Colour figure can be viewed at wileyonlinelibrary.com].

miR3954 triggers the biogenesis of 21-nt phasiRNAs from target genes

It has been reported that 22-nt miRNAs are capable of triggering the generation of phasiRNAs (Chen *et al.*, 2010). Generally, these phasiRNAs were produced in two forms: 21 nt and 24 nt (Allen *et al.*, 2005; Yoshikawa *et al.*, 2005; Johnson *et al.*, 2009; Zhai *et al.*, 2015). To evaluate whether target genes of miR3954 are potential *PHAS* loci generating phasiRNAs, we used our previously published sRNA data (Liu *et al.*, 2014b) to calculate the phasing score of all target transcripts according to a previous algorithm (De Paoli *et al.*, 2009; Xia *et al.*, 2013). Consequently, the phasing scores of all targets were > 15 (considered as valid *PHAS* loci) in all tissues when we set the phase cycle length as 21 nt (Figure 2). The phasing scores of all targets were extremely low when we set the phase cycle length as 24 nt (Figure S1). These analyses indicated that *Cs1 g09600*, *Cs1 g09635* and *Cs7 g22460* were all *PHAS* loci producing 21-nt phasiRNAs in citrus. We computationally obtained all potential 21-nt phasiRNAs produced after the miR3954 cleavage site of each target gene. Twenty-five, 20 and 22 phasiRNAs were identified from *Cs1 g09600*, *Cs1 g09635* and *Cs7 g22460*, respectively (Table S1).

Here, we termed these phasiRNAs following the previously reported nomenclature that identified the polarity and the number of hypothetical DCL processing cycles from the miRNA target site (Allen *et al.*, 2005). For instance, Cs1 g09600 3′D1(+) stands for phasiRNAs generated from the sense strand (miR3954-targeted strand) of the 1st duplex that is processed towards the 3′ terminal of *Cs1 g09600*. In general, these phasiRNAs from the same transcript had a similar distribution pattern in different tissues, such as phasiRNAs from the 3rd and 7th site of *Cs1 g09635*, which were the two most abundant phasiRNAs in all tissues (Figure 2;

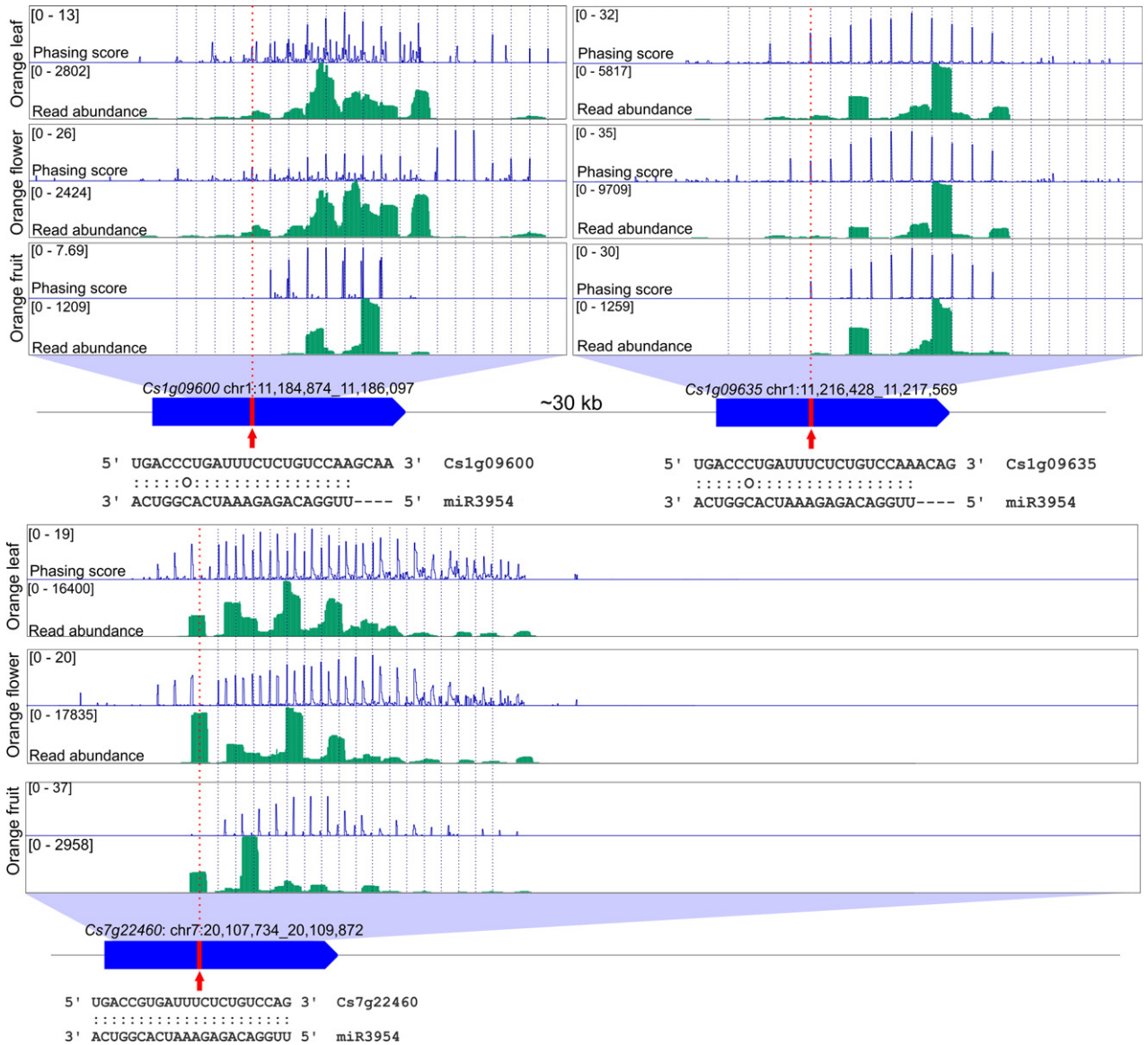

Figure 2. The 21-nt phasing score and sRNA abundance distribution along *Cs1 g09600*, *Cs1 g09635* and *Cs7 g22460* in orange leaf, flower and fruit tissues. miR3954 phasing scores were evaluated based on the mapping results of 21-nt sRNAs. The length of intervals between dotted lines is 21 nt. The miR3954-mediated cleavage sites of each target transcript are indicated by the red dotted lines and the red arrows. Genomic configurations of each target are shown at the bottom of each panel.

Table S1). Noticeably, *Cs1 g09635* had a higher phasing score and lower noise compared with other target transcripts, which indicated *Cs1 g09635* was a high confident *PHAS* locus specifically triggered by miR3954 (Figure 2). In total, eight phasiRNAs with an abundant expression level (> 100 reads in orange flower) from two lncRNA targets were selected and studied further. They were 3′D1(+), 3′D3(−), 3′D4(−), 3′D6(−) and 3′D8(−) of *Cs1 g09600*, and 3′D1(+), 3′D3(−), 3′D6(−) and 3′D7(+) of *Cs1 g09635*. Particularly, Cs1 g09635 3′D6(−) and Cs1 g09600 3′D6(−) had the same mature sequence (Table S1).

A tobacco-based transient expression system was used to confirm that miR3954 could trigger the production of phasiRNAs by targeting and cleaving *Cs1 g09600* and *Cs1 g09635*, as miR3954 is a less-conserved miRNA (it is conserved only in several species, such as peach, apple and potato, and it is also called miR7122) and its targets *Cs1 g09600* and *Cs1 g09635* are citrus-specific transcripts (i.e. both miR3954 and its non-coding targets are non-conserved in tobacco). In this assay, we used *Agrobacterium tumefaciens* infiltration to transiently co-overexpress miR3954 and its target transcripts (*Cs1 g09600* and *Cs1 g09635*) in tobacco leaves. Three days after infiltration, we checked whether the predicted phasiRNAs were produced by RNA gel blot analysis. Leaves of wild plants (WT) and leaves that overexpressed only the *MIRNA* (OX-

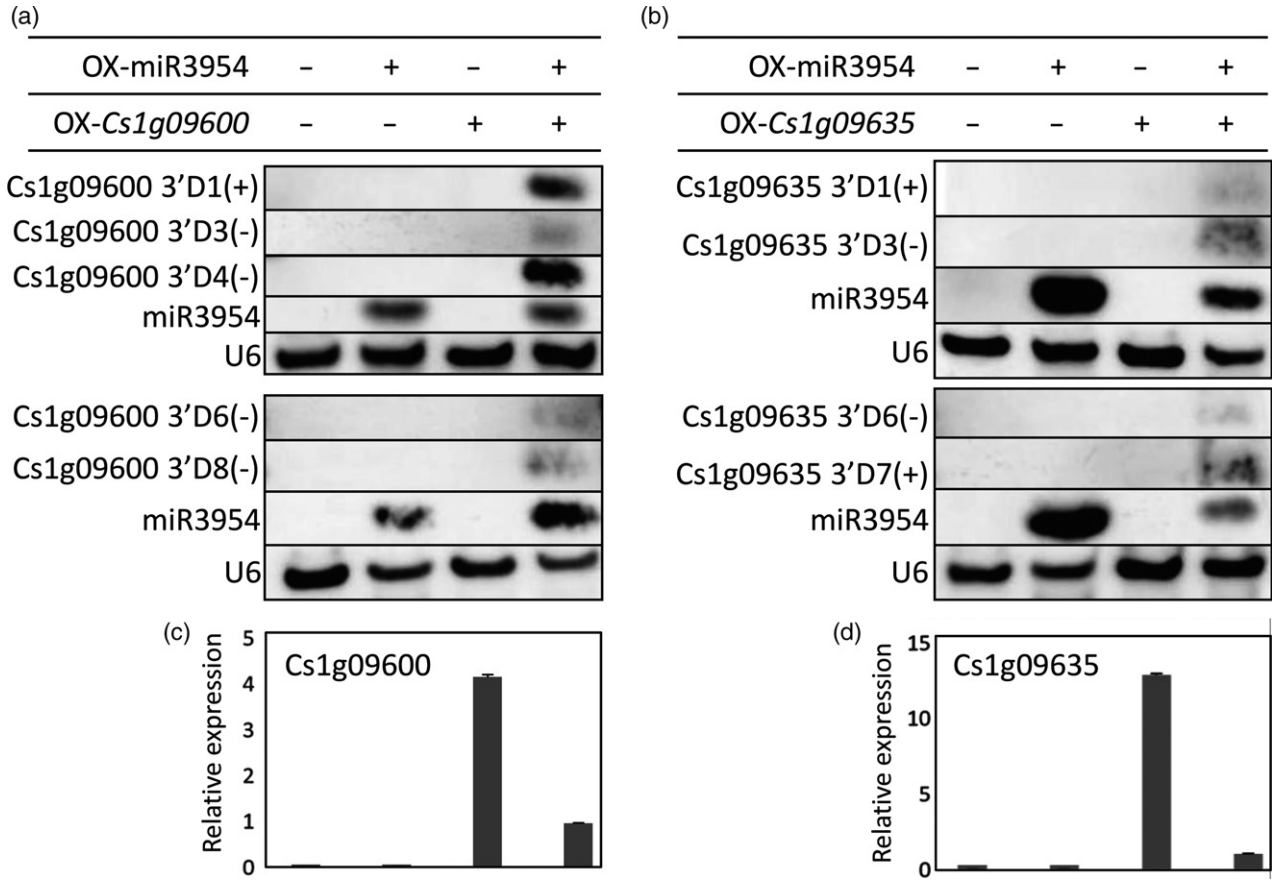

Figure 3. miR3954 targets *Cs1 g09600* and *Cs1 g09635* and triggers the biogenesis of phasiRNAs.
The tables at the top of the figure indicate the *Agrobacterium tumefaciens* expression vectors used in transient infiltration. From left to right, each lane contains total RNAs extracted from wild-type (WT) tobacco leaves, OX-miR3954 leaves, OX-*Cs1 g09600*/*Cs1 g09635* leaves and co-overexpression leaves. The expression of miR3954 and relevant phased small interfering (phasi)RNAs were analyzed by RNA gel blot. The probes used in each analysis are listed on the left. The snRNA U6 was used as a loading control. The expression of two lncRNAs was analyzed by quantitative reverse transcriptase-polymerase chain reaction (qRT-PCR), and the *actin* gene was used as a loading control. Data from the qRT-PCR experiments are represented as the mean of four biological replicates (error bars indicate the standard deviation).

miR3954) or only the target genes (OX-*Cs1 g09600*/*Cs1 g09635*) were used as negative controls. As a result, in the absence of miR3954, overexpression of *Cs1 g09600* and *Cs1 g09635* in tobacco leaves did not generate phasiRNAs (Figure 3). In contrast, all eight phasiRNAs were detected in co-overexpression leaves (Figure 3), demonstrating that miR3954 triggered the formation of phasiRNAs from both *Cs1 g09600* and *Cs1 g09635*.

Downstream target genes of phasiRNAs

To explore the downstream pathways regulated by these phasiRNAs, we identified the target genes of these phasiRNAs across the genome using the degradome data (Liu *et al.*, 2014b). We identified 35 target genes supported by the degradome data in addition to the *cis*-targeting cognate genes *Cs1 g09600*, *Cs1 g09635* and their homologs (Table S2). Following criteria previously reported (Addo-Quaye *et al.*, 2008, 2009), we divided 35 targets identified from degradome into three categories with different confidence levels. Seven of these targets were grouped into category I (highest confidence level), five were grouped into category II (inferior confidence level) and the rest were grouped into category III (lowest confidence level). The following annotation indicated that these target genes were involved in many aspects of biological processes (Table S2). Interestingly, Cs1 g09635 3′D6(−) was predicted to target eight NAC domain-containing genes, including *Cs7 g22420*, *Cs7 g22430*, *Cs7 g22450*, *Cs7 g22460*, *Cs7 g22470*, *Cs7 g22540*, *Cs7 g22560* and *orange1.1t05093*. Most of these *NAC* genes had a high confidence level (three belong to category I, two belong to category II, and three belong to category III; Figure S2; Table S2) in degradome data and a low penalty for pairing with Cs1 g09635 3′D6(−), significantly indicating that Cs1 g09635 3′D6(−) might function by targeting *NAC* transcript factors in sweet orange.

Figure 4. Target validation of Cs1 g09635 3′D6(−) in orange flower.
The 5′ rapid amplification of cDNA ends (RACE) analysis was carried out to verify the *NAC* targets of Cs1 g09635 3′D6(−). The arrows indicate the cleavage sites in each target, and the numbers indicate the frequency of valid sequenced clones.

Moreover, 5′ RACE was carried out to confirm whether these *NAC* transcripts were cleaved at the target site of Cs1 g09635 3′D6(−). Because the trigger miRNA of Cs1 g09635 3′D6(−), miR3954, was highly expressed in orange flowers, we performed the 5′ RACE analysis in orange flowers. Consequently, our analysis demonstrated that six of these *NAC* transcripts were cleaved at the target site of Cs1 g09635 3′D6(−) in orange (Figure 4). Because the sequences of *Cs7 g22430* and *Cs7 g22450* are extremely similar, it is hard to design specific 5′ RACE primers to distinguish *Cs7 g22430* from *Cs7 g22450*. We used the same 5′ RACE primer to identify the cleavage site on *Cs7 g22430* and *Cs7 g22450*; as a result, we obtained only one Cs1 g09635 3′D6(−)-mediated cleavage in *Cs7 g22430* (Figure 4).

Overexpression of miR3954 promotes the early flowering in citrus

To gain insight into the biological function of miR3954 in citrus, we generated transgenic citrus overexpression lines, in which miR3954 was driven by a constitutively active 35S promoter. Because of the advantage of its short juvenile stage (Zhang *et al.*, 2009), Hongkong kumquat (*F. hindsii*) was used as an explant for transgenic experiments in this study.

After polymerase chain reaction (PCR) confirmation with a forward primer in the 35S promoter and a reverse primer in *MIR3954*, nine independent miR3954-overexpressing lines (OX-miR3954) were validated as transgenic lines (Figure S3). Quantitative reverse transcriptase (qRT)-PCR and RNA blot hybridization showed that the expression of miR3954 was greatly elevated to varying degrees in all the transgenic lines except OX-miR3954-2 line (Figure 5a). We did not observe any notable phenotypic differences during fruit development in the OX-miR3954 lines compared with WT Hongkong kumquat. Then we sowed seeds from OX-miR3954 and WT Hongkong kumquat in the greenhouse under the same conditions. OX-miR3954 seedlings did not exhibit an observable phenotype in seed germination and vegetative growth compared with WT seedlings. However, the progenies of OX-miR3954-3, OX-miR3954-5 and OX-miR3954-7 blossomed or fruited at 7 months after seeding in the greenhouse, while the progenies of WT did not show any signs of flowering at that time (Figure 5b). Fourteen months after seeding, all these progenies of OX-miR3954 lines were fruited (Figure 5c). Later, we harvested and sowed more seeds from OX-miR3954-3, -5, -7 and WT, and evaluated the flowering time of each plant by the leaf number at the initial flowering stage. On average, OX-miR3954-3 flowered with 18.5 leaves, OX-miR3954-5 with 19.1 leaves, OX-miR3954-7 with 18.4 leaves, whereas WT flowered with 35.4 leaves (Table S3). These observations indicated that overexpression of miR3954 significantly shortened the flowering time, accelerating the transition from vegetative growth to reproductive growth.

Abundance of miR3954, phasiRNAs and their target genes in the transgenic citrus

To investigate how the overexpression of miR3954 affects downstream target genes in the transgenic plants of Hongkong kumquat, the orthologs of *Cs1 g09600* and *Cs1 g09635* in Hongkong kumquat were cloned and designated as *Fhi-09600* and *Fhi-09635*. Gene expression analysis indicated that only *Cs1 g09635* was transcribed in a relatively low level (Figure S4a). Sequence comparison showed that the transcript sequence of *Fhi-09635* was nearly identical (97% identity) to *Cs1 g09635*, completely identical (100%) in the region that generated phasiRNAs (Figure S4b).

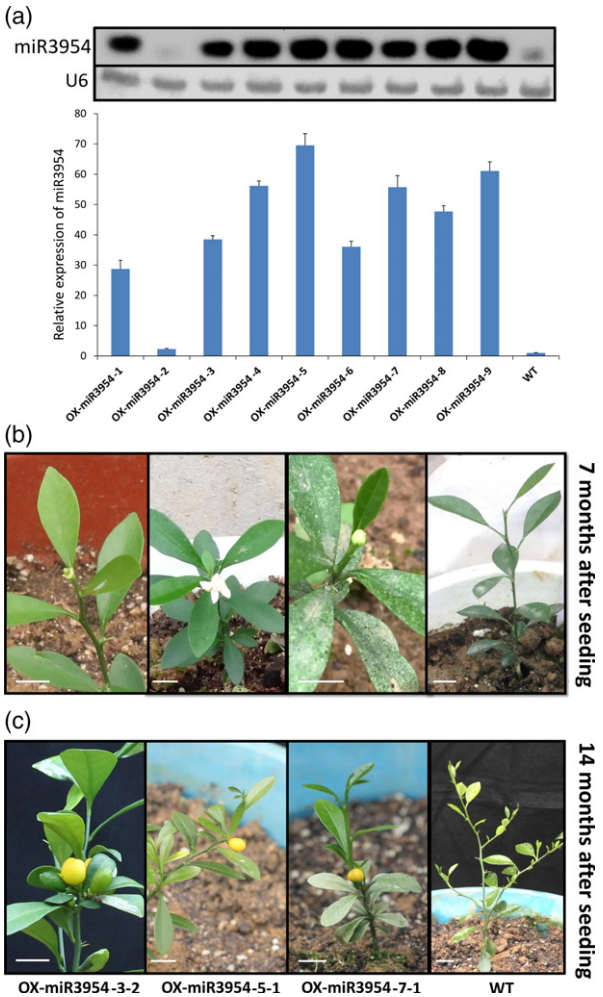

Figure 5. Transgenic overexpression of miR3954 accelerates flowering in citrus.
(a) The expression level of miR3954 in each transgenic line. The expression level was analyzed by an RNA gel blot and quantitative reverse transcriptase-polymerase chain reaction (qRT-PCR), respectively. snRNA U6 was used as a loading control in both analyses. Data from the qRT-PCR experiments are represented as the mean of three biological replicates (error bars indicate the standard deviation).
Early flowering (b) and fruiting (c) of miR3954 overexpression lines in the greenhouse. Left panels show individual progenies of OX-miR3954-3, OX-miR3954-5 or OX-miR3954-7, and the right panels show the wild-type (WT) kumquat progenies growing in the greenhouse. Seeding dates are also listed on the right side. Scale bars: 1 cm.

We examined the abundance of miR3954 target genes (*Fhi-09635* and *Fhi-22460*), phasiRNAs derived from *Fhi-09635* [Fhi-09635 3′D1(+), Fhi-09635 3′D3(−), Fhi-09635 3′D6(−) and Fhi-09635 3′D7(+)] as well as *NAC* targets of Fhi-09635 3′D6(−) in the flowers of OX-miR3954-3, -5, -7 and WT Hongkong kumquat. The expression levels of *Fhi-09635* and *Fhi-22460* were decreased in all OX-miR3954 lines that were inversely correlated with the expression pattern of miR3954 (Figures 5a and 6a). The abundance of downstream phasiRNAs was elevated, and ranged from twofold to sevenfold in different OX-miR3954 lines (Figures S5 and 6b). The observation that the elevated level of phasiRNAs (twofold to sevenfold; Figures S5 and 6b) was not as high as the elevated level of miR3954 (more than 30-fold; Figure 5a and b) was likely because the miRNA target gene (*Fhi-09635* or *Cs1 g09635*) was not co-overexpressed in our transgenic lines. As mentioned above, the sequences of *Cs7 g22430* and *Cs7 g22450* were extremely similar; we used a pair of universal primers to detect the expression level of *Cs7 g22430* and *Cs7 g22450*. Consequently, decreased levels of *Fhi-22430*, *Fhi-22450*, *Fhi-22460* and *Fhi-22470* were observed in all OX-miR3954 lines, whereas *Fhi-22420*, *Fhi-22540*, *Fhi-22560* and *Fhi-05093* did not exhibit a significant decrease between the OX-miR3954 lines and WT (Figure 6c).

DISCUSSION

To date, many 22-nt miRNAs were reported as triggers of phasiRNAs in diverse plant species and were involved in different regulatory pathways. The regulatory network mediated by miRNA and relevant phasiRNAs can be roughly summarized in Figure 7a. Initially, miRNAs trigger lncRNAs to produce phasiRNAs that turn on the *in trans* regulation. A classic pathway is the miR390-*TAS3* (lncRNA)-tasiRNAs-*ARFs*, which is widely conserved across a broad range of plants from mosses to seed plants (Williams *et al.*, 2005; Axtell *et al.*, 2006; Heisel *et al.*, 2008; Xia *et al.*, 2017). Additionally, miR2118 and miR2275 target lncRNAs and trigger the biogenesis of 21-nt phasiRNAs and 24-nt phasiRNAs, respectively, in rice (Johnson *et al.*, 2009; Song *et al.*, 2012). In Arabidopsis, miR173 targets *TAS1* and *TAS2* (lncRNAs), and triggers the formation of phasiRNAs (Chen *et al.*, 2005; Yoshikawa *et al.*, 2005). miR828-directed tasiRNAs derived from *TAS4* (lncRNA) regulate *MYBs* (Rajagopalan *et al.*, 2006). Alternatively, miRNAs target protein-coding genes as well to generate phasiRNAs that turn on both *in cis* and *in trans* regulation (Figure 7a; Howell *et al.*, 2007; Zhai *et al.*, 2011; Xia *et al.*, 2012; Zhu *et al.*, 2012). For example, the miR828-*MYBs* pathway was conserved in Rosaceae (Xia *et al.*, 2012; Zhu *et al.*, 2012). PhasiRNAs triggered by different miRNAs (miR482, miR2118 and miR1507) were generated from nucleotide binding site-leucine-rich repeat genes (*NB-LRRs*) in Solanaceae, Brassicaceae, Fabaceae and Rosaceae (Zhai *et al.*, 2011; Li *et al.*, 2012; Shivaprasad *et al.*, 2012; Fei *et al.*, 2015; Zhao *et al.*, 2015). PhasiRNA mediating *in cis* regulation may dramatically amplify the suppressive functions of their trigger miRNAs (Zhai *et al.*, 2011; Xia *et al.*, 2012; Fei *et al.*, 2013).

In this study, our findings revealed a citrus-specific pathway composed of miRNA, phasiRNAs and NAC transcription factors (Figure 7b). Our data demonstrated that the citrus 22-nt miR3954 targeted two lncRNAs (*Cs1 g09600* and *Cs1 g09635*) as well as a *NAC* transcript (*Cs7 g22460*).

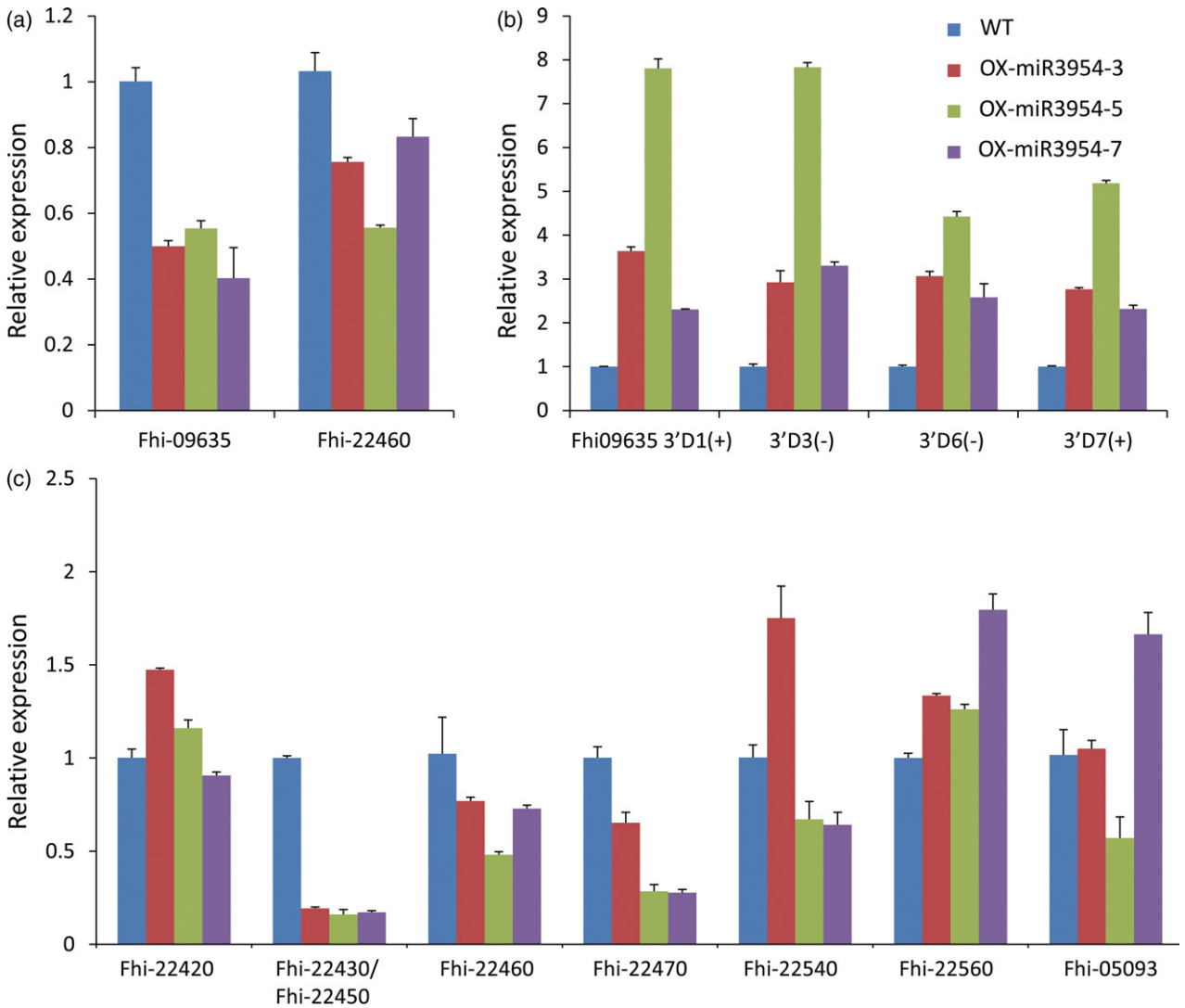

Figure 6. The expression analysis of miR3954 targets, downstream phased small interfering (phasi)RNAs and *NAC* targets of Cs1 g09635 3′D6(−) in OX-miR3954 lines and wild-type (WT).

The expression level was analyzed by quantitative reverse transcriptase-polymerase chain reaction (qRT-PCR). snRNA U6 and the *actin* gene were used as loading controls in expression analysis of phasiRNA and target genes, respectively. Data from the qRT-PCR experiments are represented as the mean of three biological replicates (error bars indicate the standard deviation).

(a) The expression analysis of miR3954 targets in OX-miR3954 lines and WT.

(b) The expression analysis of phasiRNAs from *Fhi-09635* triggered by miR3954 in OX-miR3954 lines and WT.

(c) The expression analysis of NAC target genes of Cs1 g09635 3′D6(−) in OX-miR3954 lines and WT.

We found that all three target genes generated phasiRNAs from the miR3954-mediated cleavage sites. PhasiRNAs derived from lncRNAs were remarkably abundant, while phasiRNAs derived from the *NAC* gene had a modest abundance (Table S1). *Cs1 g09600* and *Cs1 g09635* may be novel non-coding *TAS*-like (*TASL*) genes in citrus, because their phasiRNAs target *in trans* many other functional genes (Table S2). One common phasiRNA, which can be derived from both *Cs1 g09600* and *Cs1 g09635* [denoted as Cs1 g09635 3′D6(−)], targets *in trans* eight *NAC* transcripts including *Cs7 g22460* (Figure S2). Thus, we uncovered a potential regulatory network with the involvement of miR3954, its relevant phasiRNAs and *NAC* genes. In this model (Figure 7b), phasiRNAs derived from *Cs7 g22460* cannot regulate *NAC* homologs, which may be due to the fact that the *PHAS* locus in *Cs7 g22460* is not conserved with other *NACs* (Figure S6). As miR3954 targets *Cs7 g22460* with no mismatch and targets *Cs1 g09600* and *Cs1 g09635* with one mismatch (Figure 1), we hypothesize that when expressed at a low level, miR3954 prefers to target *Cs7 g22460* and generate phasiRNAs that cannot target additional *NAC* homologs. On the other hand, when

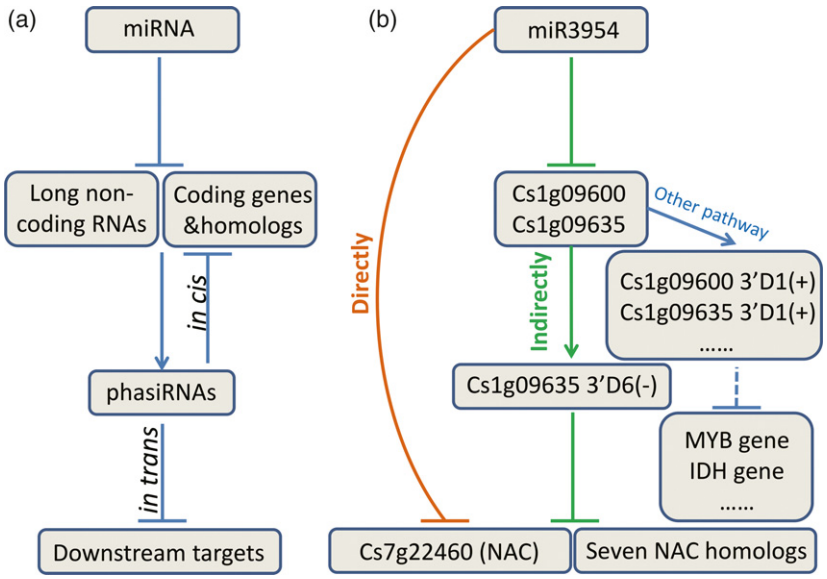

Figure 7. Summarization of different regulatory networks among miRNA, relevant phased small interfering (phasi)RNA and target genes.
(a) miRNA cleaves long non-coding RNAs or protein coding genes, and triggers the biogenesis of phasiRNAs that regulate downstream target genes. The pathway in which miRNA targets lncRNAs and turns on *in trans* regulation is also termed as the tasiRNA pathway. The pathway that miRNA cleaves protein coding genes and triggers the biogenesis of phasiRNAs amplifies the suppressive function of the trigger miRNAs (*in cis*) and *in trans* regulate downstream targets.
(b) A two-layer regulatory network of csi-miR3954 in citrus. Layer one is a direct approach (in orange color) in which miR3954 directly regulates a *NAC* gene (*Cs7 g22460*). Layer two is an indirect approach (in green color) in which miR3954 triggers the formation of Cs1 g09635 3′D6(−) by targeting two lncRNAs, and then Cs1 g09635 3′D6(−) regulates eight *NAC* homologs including *Cs7 g22460*. [Colour figure can be viewed at wileyonlinelibrary.com].

miR3954 is accumulated at a high level, the other pathway may be initiated by the redundant miR3954, resulting in the production of Cs1 g09635 3′D6(−) derived from lncRNAs. Subsequently, Cs1 g09635 3′D6(−) elevates the suppression level of *NACs* by targeting additional *NAC* homologs (Figure 7b). This hypothesized mechanism provides two different layers in repressing of *NAC* genes, directly or indirectly, which provides a more flexible and elaborate regulation of NAC transcription factors.

It is intriguing that overexpression of miR3954 leads to an early flowering phenotype in transgenic kumquat. This outcome is consistent with our observation that miR3954 has a specific expression in the flowers of sweet orange, mandarin, pummelo and kumquat (Figure 1b). Unlike the developmental defects in leaves, flowers and fruits in Arabidopsis caused by transgenic expression of miR156 and miR172 under the control of the CaMV 35S promoter (Glazinska *et al.*, 2009; Wu *et al.*, 2009; Zhu *et al.*, 2009), miR3954 only affects the transition from vegetative growth to reproductive growth in citrus. The resultant phenotype of early flowering could be caused by either direct regulation between miR3954 and *NAC* gene or by miR3954-lncRNA-phasiRNA-*NAC* pathway. In Arabidopsis, *dcl4*, *rdr6* and *sgs3* mutants that were defective in phasiRNA biogenesis exhibited accelerated vegetative phase transition (Peragine *et al.*, 2004; Xie *et al.*, 2005). This difference may be partially explained by the fact that the defects of *dcl4*, *rdr6* and *sgs3* in Arabidopsis block the biogenesis of almost all phasiRNAs, while the citrus miR3954 is specifically targeted on *NAC* genes. Our data reveal a clear clue that the *NAC* genes are vital targets of both miR3954 and phasiRNAs (Figure 4; Table S2). As expected, the high accumulation level of miR3954 arouses strong suppression of *NAC* genes (Figure 6). A previous study by overexpression of a NAC-domain protein gene (*At2 g02450*) resulted in a late-flowering phenotype (Yoo *et al.*, 2007). Therefore, it is reasonable to speculate that the suppression of *NACs* promotes early flowering in our case. It is noted that miR3954 is not conserved in Arabidopsis, but exists in many perennial plants (such as citrus, peach and apple), possibly indicating that the pathway miR3954-lcRNA/*NAC*-phasiRNA-*NAC* may affect flowering time in perennial plants.

NAC domain-containing proteins constitute one of the largest families of transcriptional factors in plants and are involved in many aspects of biological processes, including embryonic, floral and vegetative development, lateral root formation and auxin signaling, plant defense mechanisms and abiotic stress (Olsen *et al.*, 2005). Generally, miR164 targeting of a group of *NAC* genes is conserved in most plants. However, in *Populus trichocarpa*, miR6445 also targets *NACs* that do not overlap with *NACs* targeted by miR164 (Xie *et al.*, 2016). Similarly, in citrus, *NACs* targeted by miR3954 and relevant phasiRNAs are different from *NACs* targeted by miR164 (Figure S7), indicating that *NACs* regulated by miR3954 may have different functions.

In Arabidopsis, expression analyses reveal that *NAC* genes are involved in flower development and reproduction (Hu *et al.*, 2003; Hennig *et al.*, 2004; Wellmer *et al.*, 2004), and similar results were observed in rice (Kikuchi *et al.*, 2000; Fujita *et al.*, 2010). Moreover, researchers demonstrated that overexpression of a NAC-domain protein gene (*At2 g02450*) results in a late-flowering phenotype (Yoo *et al.*, 2007). All of these previous researches suggested that *NAC* genes may function as regulators in plant reproductive development. Our work provided clues about the involvement of the miR3954-phasiRNA-*NACs* pathway in citrus reproduction development. Characterizing this mechanism fully requires further functional analysis of these *NAC* genes targeted by phasiRNAs.

In conclusion, our work uncovered an intricate regulatory network that consisted of miR3954, two lncRNAs, relevant phasiRNAs and *NAC* genes. We proposed that the two layers of regulation (directly or indirectly) may provide more flexibility to the regulation of NAC genes by small RNAs. Our data also suggest that the miR3954a-mediated regulatory circuit may play a role in the induction of early flowering in citrus.

EXPERIMENTAL PROCEDURES

Plant materials

Leaf, flower and fruit of sweet orange (*C. sinensis*), pummelo (*C. grandis*), mandarin (*C. reticulata*) and Hongkong kumquat (*F. hindsii*) were collected at National Citrus Breeding Center in Huazhong Agriculture University. All samples for RNA isolation were frozen in liquid nitrogen immediately after collection and kept at −80°C until use. The *Nicotiana benthamiana* used in transient expression analysis system was planted in a growth chamber controlled at 14 h light, 10 h dark, 25°C cycles. The well-developed seeds of *F. hindsii* were collected at National Citrus Breeding Center in Huazhong Agriculture University. Epicotyls of *F. hindisii* were harvested through sterilized seeding as reported previously (Tan *et al.*, 2009). Epicotyls of *F. hindsii* were used as explant sources in citrus transformation.

Bioinformatics analysis

The secondary structure of miR3954 was predicted using RNAfold in the Vienna RNA Package as previously described (Liu *et al.*, 2014b). Data set and bioinformatics pipeline used in the identification of phasiRNAs triggered by miR3954 and their target genes were attainable from a previous publication (Liu *et al.*, 2014b). In brief, firstly, miR3954 and its target transcripts were obtained from degradome data. Secondly, all 21-nt or 24-nt standard phasiRNAs generated from the cleavage site of target transcripts to 3′ end of targets were predicted one by one. Finally, we checked the expression level and target transcripts for all predicted phasiRNAs from sRNAome and degradome data, respectively. Phasing score was calculated through the algorithm that was developed by De Paoli *et al.* (2009) and refined in Xia *et al.* (2013). Phasing score data were shown using Integrative Genomics Viewer (Robinson *et al.*, 2011). Gene coding potential was calculated by Coding Potential Calculator online (http://cpc.cbi.pku.edu.cn/; Kong *et al.*, 2007).

Expression analyses of small RNAs and their target genes

To analyze expression levels of miRNAs and phasiRNAs, stem-loop qRT-PCR and RNA gel blot analysis were both used in this study. In both analyses spliceosomal snRNA U6 was used as internal control (Kou *et al.*, 2012). Stem-loop qRT-PCR was performed referring to the previously published method (Chen *et al.*, 2005; Varkonyi-Gasic *et al.*, 2007). Stem-loop RT primers and qPCR primers for miR3954, phasiRNAs and U6 were listed in Table S4. U6 was reversely transcribed by its reverse primer, which was also used in the qPCR reaction. Small RNA gel blot analysis was performed as described previously (Liu *et al.*, 2014b). Specific probes were designed for all sRNAs and U6. The sequences of probes were listed in Table S5. To analyze expression levels of target genes of sRNAs, qRT-PCR was performed where *Actin* gene was used as a loading control. All target genes were reversely transcribed using random primers/oligo dT primer mix. The primers for target genes used in the qRT-PCR analysis were designed to encompass the cleavage sites mediated by miR3954 or phasiRNAs. The sequences information of primers was listed in Table S6.

Target gene validation

To verify the cleavage sites of target genes, 5′ RACE was carried out. 5′ RACE was performed using GeneRacer Kit (Invitrogen) following the manufacturer's instructions. Specific outer and inner reverse primers for each target gene used in the 5′ RACE analysis were listed in Table S7.

Cloning of *MIR3954, Cs1 g09600* and *Cs1 g09635*, and construction of overexpression vectors

We designed primers according to the orange genome to clone *MIR3954*, *Cs1 g09600* and *Cs1 g09635*. We cloned a 591-nt transcript of *MIR3954* containing the 148-nt canonical secondary structure of pre-miR3954 from orange cDNA. Subsequently, the cloned *MIR3954* was inserted into an overexpression vector. This OX-miR3954 vector was used in the transient expression in tobacco and citrus transformation. We cloned a 594-nt transcript of *Cs1 g09600* covering the cleavage site of miR3954 and all aforementioned phasiRNAs. We also cloned a 678-nt transcript of *Cs1 g09635* covering the cleavage site of miR3954 and all aforementioned phasiRNAs. These two cloned transcripts were inserted into overexpression vectors, respectively. OX-*Cs1 g09600* and OX-*Cs1 g09635* were used in transient expression assay. The detailed information of sequences was listed in Appendix S2.

Transient expression assay in tobacco

To verify miR3954-mediated cleavage on *Cs1 g09600* and *Cs1 g09635* and triggering the biogenesis of downstream phasiRNAs *in vivo*, we used *A. tumefaciens* infiltration to co-express miR3954 and its targets in tobacco leaves. Transient expression in tobacco was performed as described previously (Sparkes *et al.*, 2006). *Agrobacterium tumefaciens* GV3101 was used as the mediator in this assay.

Citrus transformation and regeneration

Agrobacterium tumefaciens EHA105 was used as the mediator in citrus transformation. The transformation and regeneration procedure were described previously (Duan *et al.*, 2007).

Cloning orthologous genes from Hongkong kumquat

As Hongkong kumquat is closely related with Citrus and belongs to the Citrinae group of the subfamily Aurantioideae in Rutaceae family (Swingle, 1967), primers designed for sweet orange were directly used to clone the orthologs of *Cs1 g09600*, *Cs1 g09635* and *NACs* in Hongkong kumquat. After that, we sequenced all the orthologs in Hongkong kumquat. Based on the sequence information, we designed primers of *Fhi-09600*, *Fhi-09635* and *Fhi-NACs* to perform subsequent qRT-PCR analysis.

ACKNOWLEDGEMENTS

This work was funded by the National Natural Science Foundation of China (31572105 and 31521092) and the key project of Hubei provincial Natural Science Foundation (2015CFA031).

CONFLICT OF INTEREST

The authors declare no conflict of interest.

SUPPORTING INFORMATION

Additional Supporting Information may be found in the online version of this article.

Figure S1. 24-nt phasing score distribution along *Cs1 g09600*, *Cs1 g09635* and *Cs7 g22460* in orange leaf, flower and fruit tissues.

Figure S2. T-plots of the *NAC* targets of Cs1 g09635 3′D6(−).

Figure S3. Genotyping of miR3954 transgenic lines.

Figure S4. Comparison of non-coding targets of miR3954 in orange and kumquat.

Figure S5. The expression analysis of phasiRNAs from *Fhi-09635* in OX-miR3954 lines and WT.

Figure S6. *PHAS* locus in *Cs7 g22460*.

Figure S7. Comparison of miR3954 and miR164 targeted *NACs*.

Table S1. Reads of all phasiRNAs derived from *Cs1 g09600*, *Cs1 g09635* and *Cs7 g22460* in different orange tissues

Table S2. Annotation of targets of phasiRNAs derived from *Cs1 g09600* and *Cs1 g09635*

Table S3. The flowering times of OX-miR3954 lines and WT kumquat

Table S4. Primers for qRT-PCR of small RNAs

Table S5. Probes used in the sRNA gel blot

Table S6. Primers for qRT-PCR of target genes

Table S7. Inner and outer primers for 5′ RACE analysis of target genes

Appendix S1. Coding potential analyses of *Cs1 g09600* and *Cs1 g09635*.

Appendix S2. Detailed information about sequences used in the construction of overexpression vectors.

REFERENCES

Addo-Quaye, C., Eshoo, T.W., Bartel, D.P. and Axtell, M.J. (2008) Endogenous siRNA and miRNA targets identified by sequencing of the *Arabidopsis* degradome. *Curr. Biol.* **18**, 758–762.

Addo-Quaye, C., Miller, W. and Axtell, M.J. (2009) CleaveLand: a pipeline for using degradome data to find cleaved small RNA targets. *Bioinformatics*, **25**, 130–131.

Allen, E. and Howell, M.D. (2010) miRNAs in the biogenesis of trans-acting siRNAs in higher plants. *Semin. Cell Dev. Biol.* **21**, 798–804.

Allen, E., Xie, Z., Gustafson, A.M. and Carrington, J.C. (2005) microRNA-directed phasing during trans-acting siRNA biogenesis in plants. *Cell*, **121**, 207–221.

Arikit, S., Xia, R., Kakrana, A., *et al.* (2014) An atlas of soybean small RNAs identifies phased siRNAs from hundreds of coding genes. *Plant Cell*, **26**, 4584–4601.

Axtell, M.J., Jan, C., Rajagopalan, R. and Bartel, D.P. (2006) A two-hit trigger for siRNA biogenesis in plants. *Cell*, **127**, 565–577.

Bartel, D.P. (2004) MicroRNAs: genomics, biogenesis, mechanism, and function. *Cell*, **116**, 281–297.

Chen, C., Ridzon, D.A., Broomer, A.J., *et al.* (2005) Real-time quantification of microRNAs by stem-loop RT-PCR. *Nucleic Acids Res.* **33**, e179.

Chen, H., Chen, L., Patel, K., Li, Y., Baulcombe, D.C. and Wu, S. (2010) 22-Nucleotide RNAs trigger secondary siRNA biogenesis in plants. *Proc. Natl Acad. Sci. USA*, **107**, 15269–15274.

Cho, S.H., Coruh, C. and Axtell, M.J. (2012) miR156 and miR390 regulate tasiRNA accumulation and developmental timing in *Physcomitrella patens*. *Plant Cell*, **24**, 4837–4849.

Cuperus, J.T., Carbonell, A., Fahlgren, N., Garcia-Ruiz, H., Burke, R.T., Takeda, A., Sullivan, C.M., Gilbert, S.D., Montgomery, T.A. and Carrington, J.C. (2010) Unique functionality of 22-nt miRNAs in triggering RDR6-dependent siRNA biogenesis from target transcripts in *Arabidopsis*. *Nat. Struct. Mol. Biol.* **17**, 997–1003.

De Paoli, E., Dorantes-Acosta, A., Zhai, J., Accerbi, M., Jeong, D.-H., Park, S., Meyers, B.C., Jorgensen, R.A. and Green, P.J. (2009) Distinct extremely abundant siRNAs associated with cosuppression in petunia. *RNA*, **15**, 1965–1970.

Duan, Y., Liu, X., Fan, J., Li, D., Wu, R. and Guo, W. (2007) Multiple shoot induction from seedling epicotyls and transgenic citrus plant regeneration containing the green fluorescent protein gene. *Bot. Stud.* **48**, 165–171.

Fei, Q., Xia, R. and Meyers, B.C. (2013) Phased, secondary, small interfering RNAs in posttranscriptional regulatory networks. *Plant Cell*, **25**, 2400–2415.

Fei, Q., Li, P., Teng, C. and Meyers, B.C. (2015) Secondary siRNAs from Medicago NB-LRRs modulated via miRNA–target interactions and their abundances. *Plant J.* **83**, 451–465.

Fujita, M., Horiuchi, Y., Ueda, Y., Mizuta, Y., Kubo, T., Yano, K., Yamaki, S., Tsuda, K., Nagata, T. and Niihama, M. (2010) Rice expression atlas in reproductive development. *Plant Cell Physiol.* **51**, 2060–2081.

Glazinska, P., Zienkiewicz, A., Wojciechowski, W. and Kopcewicz, J. (2009) The putative miR172 target gene *InAPETALA2*-like is involved in the photoperiodic flower induction of *Ipomoea nil*. *J. Plant Physiol.* **166**, 1801–1813.

Heisel, S.E., Zhang, Y., Allen, E., Guo, L., Reynolds, T.L., Yang, X., Kovalic, D. and Roberts, J.K. (2008) Characterization of unique small RNA populations from rice grain. *PLoS ONE*, **3**, e2871.

Hennig, L., Gruissem, W., Grossniklaus, U. and Köhler, C. (2004) Transcriptional programs of early reproductive stages in *Arabidopsis*. *Plant Physiol.* **135**, 1765–1775.

Howell, M.D., Fahlgren, N., Chapman, E.J., Cumbie, J.S., Sullivan, C.M., Givan, S.A., Kasschau, K.D. and Carrington, J.C. (2007) Genome-wide analysis of the *RNA-DEPENDENT RNA POLYMERASE6/DICER-LIKE4* pathway in *Arabidopsis* reveals dependency on miRNA-and tasiRNA-directed targeting. *Plant Cell*, **19**, 926–942.

Hu, W., Wang, Y., Bowers, C. and Ma, H. (2003) Isolation, sequence analysis, and expression studies of florally expressed cDNAs in *Arabidopsis*. *Plant Mol. Biol.* **53**, 545–563.

Johnson, C., Kasprzewska, A., Tennessen, K., Fernandes, J., Nan, G.L., Walbot, V., Sundaresan, V., Vance, V. and Bowman, L.H. (2009) Clusters and superclusters of phased small RNAs in the developing inflorescence of rice. *Genome Res.* **19**, 1429–1440.

Kikuchi, K., Ueguchi-Tanaka, M., Yoshida, K., Nagato, Y., Matsusoka, M. and Hirano, H.-Y. (2000) Molecular analysis of the *NAC* gene family in rice. *Mol. Gen. Genet.* **262**, 1047–1051.

Kong, L., Zhang, Y., Ye, Z.-Q., Liu, X.-Q., Zhao, S.-Q., Wei, L. and Gao, G. (2007) CPC: assess the protein-coding potential of transcripts using sequence features and support vector machine. *Nucleic Acids Res.***35**, W345–W349.

Kou, S.J., Wu, X., Liu, Z., Liu, Y., Xu, Q. and Guo, W. (2012) Selection and validation of suitable reference genes for miRNA expression

normalization by quantitative RT-PCR in citrus somatic embryogenic and adult tissues. *Plant Cell Rep.* **31**, 2151–2163.

Lam, P., Zhao, L., Eveleigh, N., Yu, Y., Chen, X. and Kunst, L. (2015) The exosome and trans-acting small interfering RNAs regulate cuticular wax biosynthesis during Arabidopsis inflorescence stem development. *Plant Physiol.* **167**, 323–336.

Li, F., Pignatta, D., Bendix, C., Brunkard, J.O., Cohn, M.M., Tung, J., Sun, H., Kumar, P. and Baker, B. (2012) MicroRNA regulation of plant innate immune receptors. *Proc. Natl Acad. Sci. USA*, **109**, 1790–1795.

Li, S., Liu, J., Liu, Z., Li, X., Wu, F. and He, Y. (2014) *HEAT-INDUCED TAS1 TARGET1* mediates thermotolerance via HEAT STRESS TRANSCRIPTION FACTOR A1a-directed pathways in *Arabidopsis*. *Plant Cell*, **26**, 1764–1780.

Liu, B., Chen, Z., Song, X., Liu, C., Cui, X., Zhao, X., Fang, J., Xu, W., Zhang, H. and Wang, X. (2007) *Oryza sativa dicer-like4* reveals a key role for small interfering RNA silencing in plant development. *Plant Cell*, **19**, 2705–2718.

Liu, Q., Wang, F. and Axtell, M.J. (2014a) Analysis of complementarity requirements for plant microRNA targeting using a *Nicotiana benthamiana* quantitative transient assay. *Plant Cell*, **26**, 741–753.

Liu, Y., Wang, L., Chen, D., Wu, X., Huang, D., Chen, L., Li, L., Deng, X. and Xu, Q. (2014b) Genome-wide comparison of microRNAs and their targeted transcripts among leaf, flower and fruit of sweet orange. *BMC Genom.* **15**, 695.

Llave, C., Xie, Z., Kasschau, K.D. and Carrington, J.C. (2002) Cleavage of Scarecrow-like mRNA targets directed by a class of *Arabidopsis* miRNA. *Science*, **297**, 2053–2056.

Mallory, A.C. and Bouché, N. (2008) MicroRNA-directed regulation: to cleave or not to cleave. *Trends Plant Sci.* **13**, 359–367.

Montgomery, T.A., Howell, M.D., Cuperus, J.T., Li, D., Hansen, J.E., Alexander, A.L., Chapman, E.J., Fahlgren, N., Allen, E. and Carrington, J.C. (2008) Specificity of ARGONAUTE7-miR390 interaction and dual functionality in TAS3 trans-acting siRNA formation. *Cell*, **133**, 128–141.

Olsen, A.N., Ernst, H.A., Leggio, L.L. and Skriver, K. (2005) *NAC* transcription factors: structurally distinct, functionally diverse. *Trends Plant Sci.* **10**, 79–87.

Pan, Z., Liu, Q., Yun, Z., Guan, R., Zeng, W., Xu, Q. and Deng, X. (2009) Comparative proteomics of a lycopene-accumulating mutant reveals the important role of oxidative stress on carotenogenesis in sweet orange (Citrus sinensis [L.] osbeck). *Proteomics*, **9**, 5455–5470.

Pan, Z., Zeng, Y., An, J., Ye, J., Xu, Q. and Deng, X. (2012) An integrative analysis of transcriptome and proteome provides new insights into carotenoid biosynthesis and regulation in sweet orange fruits. *J. Proteomics.* **75**, 2670–2684.

Peragine, A., Yoshikawa, M., Wu, G., Albrecht, H.L. and Poethig, R.S. (2004) *SGS3* and *SGS2/SDE1/RDR6* are required for juvenile development and the production of trans-acting siRNAs in *Arabidopsis*. *Genes Dev.* **18**, 2368–2379.

Rajagopalan, R., Vaucheret, H., Trejo, J. and Bartel, D.P. (2006) A diverse and evolutionarily fluid set of microRNAs in *Arabidopsis thaliana*. *Genes Dev.* **20**, 3407–3425.

Robinson, J.T., Thorvaldsdóttir, H., Winckler, W., Guttman, M., Lander, E.S., Getz, G. and Mesirov, J.P. (2011) Integrative genomics viewer. *Nat. Biotechnol.* **29**, 24–26.

Rock, C.D. (2013) Trans-acting small interfering RNA4: key to nutraceutical synthesis in grape development? *Trends Plant Sci.* **18**, 601–610.

Shivaprasad, P.V., Chen, H.-M., Patel, K., Bond, D.M., Santos, B.A. and Baulcombe, D.C. (2012) A microRNA superfamily regulates nucleotide binding site–leucine-rich repeats and other mRNAs. *Plant Cell*, **24**, 859–874.

Song, X., Li, P., Zhai, J., Zhou, M., Ma, L., Liu, B., Jeong, D.H., Nakano, M., Cao, S. and Liu, C. (2012) Roles of *DCL4* and *DCL3b* in rice phased small RNA biogenesis. *Plant J.* **69**, 462–474.

Sparkes, I.A., Runions, J., Kearns, A. and Hawes, C. (2006) Rapid, transient expression of fluorescent fusion proteins in tobacco plants and generation of stably transformed plants. *Nat. Protoc.* **1**, 2019–2025.

Swingle, W.T. (1967) The botany of Citrus and its wild relatives. In *The Citrus Industry* (Reuther, W., Webber, H.J. and Batchelor, L.D. eds). Berkeley, CA: University of California Press, pp. 190–430.

Tan, B., Li, D., Xu, S., Fan, G., Fan, J. and Guo, W. (2009) Highly efficient transformation of the *GFP* and *MAC12. 2* genes into *precocious trifoliate* orange (*Poncirus trifoliata* [L.] Raf), a potential model genotype for functional genomics studies in Citrus. *Tree Genet. Genomes*, **5**, 529–537.

Varkonyi-Gasic, E., Wu, R., Wood, M., Walton, E.F. and Hellens, R.P. (2007) Protocol: a highly sensitive RT-PCR method for detection and quantification of microRNAs. *Plant Methods*, **3**, 12.

Vaucheret, H. (2008) Plant argonautes. *Trends Plant Sci.* **13**, 350–358.

Vazquez, F., Vaucheret, H., Rajagopalan, R., Lepers, C., Gasciolli, V., Mallory, A.C., Hilbert, J.-L., Bartel, D.P. and Crété, P. (2004) Endogenous trans-acting siRNAs regulate the accumulation of *Arabidopsis* mRNAs. *Mol. Cell*, **16**, 69–79.

Voinnet, O. (2009) Origin, biogenesis, and activity of plant microRNAs. *Cell*, **136**, 669–687.

Wang, H., Zhang, X., Liu, J., Kiba, T., Woo, J., Ojo, T., Hafner, M., Tuschl, T., Chua, N. and Wang, X. (2011) Deep sequencing of small RNAs specifically associated with *Arabidopsis* AGO1 and AGO4 uncovers new AGO functions. *Plant J.* **67**, 292–304.

Wellmer, F., Riechmann, J.L., Alves-Ferreira, M. and Meyerowitz, E.M. (2004) Genome-wide analysis of spatial gene expression in *Arabidopsis* flowers. *Plant Cell*, **16**, 1314–1326.

Williams, L., Carles, C.C., Osmont, K.S. and Fletcher, J.C. (2005) A database analysis method identifies an endogenous trans-acting short-interfering RNA that targets the *Arabidopsis ARF2, ARF3*, and *ARF4* genes. *Proc. Natl Acad. Sci. USA*, **102**, 9703–9708.

Wu, G., Park, M.Y., Conway, S.R., Wang, J.W., Weigel, D. and Poethig, R.S. (2009) The sequential action of miR156 and miR172 regulates developmental timing in *Arabidopsis*. *Cell*, **138**, 750–759.

Wu, X., Kou, S., Liu, Y., Fang, Y., Xu, Q. and Guo, W. (2015) Genomewide analysis of small RNAs in nonembryogenic and embryogenic tissues of citrus: microRNA-and siRNA-mediated transcript cleavage involved in somatic embryogenesis. *Plant Biotechnol. J.* **13**, 383–394.

Xia, R., Zhu, H., An, Y., Beers, E.P. and Liu, Z. (2012) Apple miRNAs and tasiRNAs with novel regulatory networks. *Genome Biol.* **13**, R47.

Xia, R., Meyers, B.C., Liu, Z., Beers, E.P., Ye, S. and Liu, Z. (2013) MicroRNA superfamilies descended from miR390 and their roles in secondary small interfering RNA biogenesis in eudicots. *Plant Cell*, **25**, 1555–1572.

Xia, R., Xu, J., Arikit, S. and Meyers, B.C. (2015a) Extensive families of miRNAs and *PHAS* Loci in *Norway Spruce* demonstrate the origins of complex phasiRNA networks in seed plants. *Mol. Biol. Evol.* **32**, 2905–2918.

Xia, R., Ye, S., Liu, Z., Meyers, B.C. and Liu, Z. (2015b) Novel and recently evolved microRNA clusters regulate expansive *F-BOX* gene networks through phased small interfering RNAs in wild diploid strawberry. *Plant Physiol.* **169**, 594–610.

Xia, R., Xu, J. and Meyers, B.C. (2017) The emergence, evolution, and diversification of the miR390-TAS3-ARF pathway in land plants. *The Plant Cell, tpc.* **00185**, 02017.

Xie, Z., Allen, E., Wilken, A. and Carrington, J.C. (2005) *DICER-LIKE 4* functions in trans-acting small interfering RNA biogenesis and vegetative phase change in *Arabidopsis thaliana*. *Proc. Natl Acad. Sci. USA*, **102**, 12984–12989.

Xie, J., Yang, X., Song, Y., Du, Q., Li, Y., Chen, J. and Zhang, D. (2016) Adaptive evolution and functional innovation of *Populus*-specific recently evolved microRNAs. *New Phytolo.* **213**, 206–219.

Xu, Q., Liu, Y., Zhu, A., Wu, X., Ye, J., Yu, K., Guo, W. and Deng, X. (2010) Discovery and comparative profiling of microRNAs in a sweet orange red-flesh mutant and its wild type. *BMC Genom.* **11**, 246.

Yoo, S.Y., Kim, Y., Kim, S.Y., Lee, J.S. and Ahn, J.H. (2007) Control of flowering time and cold response by a NAC-domain protein in *Arabidopsis*. *PLoS ONE*, **2**, e642.

Yoshikawa, M., Peragine, A., Park, M.Y. and Poethig, R.S. (2005) A pathway for the biogenesis of trans-acting siRNAs in *Arabidopsis*. *Genes Dev.* **19**, 2164–2175.

Yoshikawa, M., Iki, T., Tsutsui, Y., Miyashita, K., Poethig, R.S., Habu, Y. and Ishikawa, M. (2013) 3′ fragment of miR173-programmed RISC-cleaved RNA is protected from degradation in a complex with RISC and SGS3. *Proc. Natl Acad. Sci. USA*, **110**, 4117–4122.

Zhai, J., Jeong, D.-H., De Paoli, E., Park, S., Rosen, B.D., Li, Y., González, A.J., Yan, Z., Kitto, S.L. and Grusak, M.A. (2011) MicroRNAs as master regulators of the plant *NB-LRR* defense gene family via the production of phased, trans-acting siRNAs. *Genes Dev.* **25**, 2540–2553.

Zhai, J., Zhang, H., Arikit, S., Huang, K., Nan, G.-L., Walbot, V. and Meyers, B.C. (2015) Spatiotemporally dynamic, cell-type-dependent premeiotic

and meiotic phasiRNAs in maize anthers. *Proc. Natl Acad. Sci. USA*, **112**, 3146–3151.

Zhang, J., Tao, N., Xu, Q., Zhou, W., Cao, H., Xu, J. and Deng, X. (2009) Functional characterization of *Citrus PSY* gene in Hongkong kumquat (*Fortunella hindsii* Swingle). *Plant Cell Rep.* **28**, 1737–1746.

Zhao, M., Cai, C., Zhai, J., Lin, F., Li, L., Shreve, J., Thimmapuram, J., Hughes, T.J., Meyers, B.C. and Ma, J. (2015) Coordination of microRNAs, phasiRNAs, and *NB-LRR* genes in response to a plant pathogen: insights from analyses of a set of soybean *Rps* gene near-isogenic lines. *Plant Genome*, **8**, 3835.

Zheng, B.-B., Fang, Y.-N., Pan, Z.-Y., Sun, L., Deng, X.-X., Grosser, J.W. and Guo, W.-W. (2014) iTRAQ-based quantitative proteomics analysis revealed alterations of carbohydrate metabolism pathways and mitochondrial proteins in a male sterile cybrid pummelo. *J. Proteome Res.* **13**, 2998–3015.

Zheng, Y., Wang, Y., Wu, J., Ding, B. and Fei, Z. (2015) A dynamic evolutionary and functional landscape of plant phased small interfering RNAs. *BMC Biol.* **13**, 32.

Zhu, Q., Upadhyaya, N.M., Gubler, F. and Helliwell, C.A. (2009) Over-expression of miR172 causes loss of spikelet determinacy and floral organ abnormalities in rice (*Oryza sativa*). *BMC Plant Biol.* **9**, 149.

Zhu, H., Xia, R., Zhao, B., An, Y.-Q., Dardick, C.D., Callahan, A.M. and Liu, Z. (2012) Unique expression, processing regulation, and regulatory network of peach (*Prunus persica*) miRNAs. *BMC Plant Biol.* **12**, 149.

